

5th International Conference on Silicon Photovoltaics, SiliconPV 2015

## Design of 4-terminal solar modules combining thin-film wide-bandgap top cells and c-Si bottom cells

Dong Zhang<sup>a,\*</sup>, Wim Soppe<sup>a</sup>, Ruud. E. I. Schropp<sup>a,b</sup><sup>a</sup>ECN-Solliance, High Tech Campus 21, 5656 AE Eindhoven, the Netherlands<sup>b</sup>TU/e-Solliance, Department of Applied Physics, PMP, P.O.Box 513, 5600 MB Eindhoven, the Netherlands

---

### Abstract

Optical simulations of 4-terminal hybrid tandem modules combining high-efficiency crystalline silicon (c-Si) cells with three different thin-film top cells respectively are presented. We considered three types of thin film PV cells: 1. Enlarged-bandgap oxygenated amorphous silicon (a-SiO:H) cells, 2. Wide-bandgap chalcopyrite (CuGaSe<sub>2</sub>) cells, and 3. Perovskite (CH<sub>3</sub>NH<sub>3</sub>PbI<sub>3</sub>) cells. A methodology for evaluating the efficiency gain of the 4-terminal hybrid tandem module is proposed and used to show how the efficiency of an interdigitated back contact (IBC) c-Si module with an efficiency of about 19.5% can significantly be increased through this 4-terminal tandem concept. In our model we also included the change in electrical output parameters by the color-filtering effect of the top cells.

© 2015 The Authors. Published by Elsevier Ltd. This is an open access article under the CC BY-NC-ND license (<http://creativecommons.org/licenses/by-nc-nd/4.0/>).

Peer review by the scientific conference committee of SiliconPV 2015 under responsibility of PSE AG

**Keywords:** solar module; 4-terminal; tandem; simulation

---

### 1. Introduction

For single-junction crystalline silicon (c-Si) solar cells, the previous efficiency record of 25% has been established in 1998 [1]. This record stood for 15 years until last year, when Panasonic announced their back-contacted HIT<sup>®</sup> cell that reached efficiency of 25.6% [2]. The difficulty in improving the c-Si cell efficiency inevitably limits the module efficiency (current maximum about 22%). The practical limit for single junction c-Si

---

\* Corresponding author. Tel.: +31-(0)88-515-4490; fax: +31-(0)88-515-8214.

E-mail address: [d.zhang@ecn.nl](mailto:d.zhang@ecn.nl)

modules is generally thought to be 24-25%. To surpass the practical efficiency limits of single-junction c-Si modules, 4-terminal hybrid tandem modules consisting of wide-bandgap thin-film cells and high-efficiency c-Si bottom cells have been suggested [3]. Compared to the common 2-terminal structure, the 4-terminal hybrid tandem structure has several advantages: no need of current or lattice matching, simple mechanical stacking, more freedom for choosing the top and bottom cells, and most of all the possibility to use monolithic series connection for the thin-film top cell.

In this contribution, a 4-terminal hybrid tandem module structure combining thin-film top cells and c-Si bottom cells is proposed. On the basis of a single-junction IBC module structure (Fig. 1(a)), a thin-film solar cell can be deposited and interconnected on the inner side of the module cover glass as shown in Fig. 1(b), implying a minor change of the single-junction IBC module structure. In the simulation and optical design, an IBC solar cell processed at ECN is adopted as the bottom cell. The design of three types of thin-film solar cells as the top cell has been studied, 1. enlarged-bandgap oxygenated amorphous silicon (a-SiO:H) cells, 2. Wide-bandgap chalcopyrite (CuGaSe<sub>2</sub>) cells, and 3. perovskite (CH<sub>3</sub>NH<sub>3</sub>PbI<sub>3</sub>) cells, and the potential efficiency gain is evaluated.

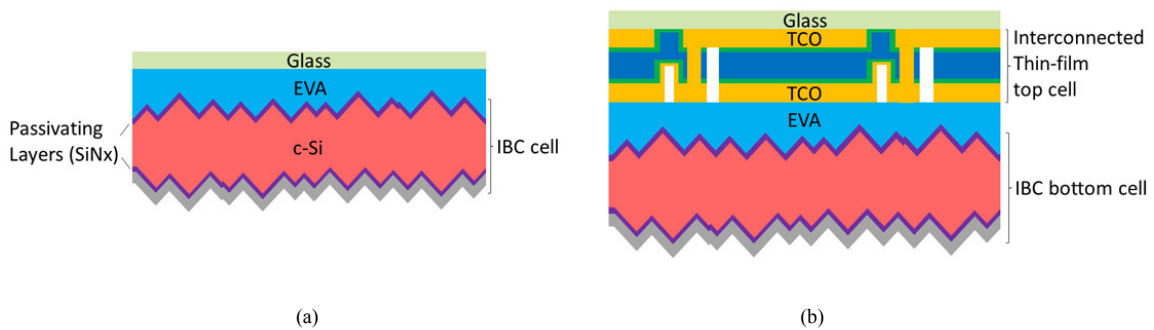


Fig. 1. Schematic layer stacks of (a) a single-junction IBC module and (b) a 4-terminal hybrid tandem module combining an interconnected thin-film top cell and a bottom IBC cell.

## 2. Optical simulation

The optical simulations are carried out with Advanced Semiconductor Analysis (ASA) software developed at Delft University of Technology [4, 5]. Both wave and geometrical optics are included. Layer geometry of solar modules and optical properties of each material are used as input. To evaluate the optical effectiveness of a certain module structure, the weighted fractional absorbance ( $\bar{A}$ ) of a layer in the solar module is defined by the equation:

$$\bar{A}(\%) = \frac{\int_{1200}^{300} A(\lambda) \phi(\lambda) d\lambda}{\int_{1200}^{300} \phi(\lambda) d\lambda}, \quad (1)$$

where  $A(\lambda)$  is the net absorbance of a layer in the solar module taking into account the transmission and reflection of all other layers in the stack,  $\phi(\lambda)$  is the photon flux of the AM1.5 solar spectrum and thereby  $\bar{A}$  indicates the fraction of the absorbed photons in the AM1.5 solar spectrum. Note that only the wavelength range of 300 nm to 1200 nm is considered since the photon flux at wavelengths shorter than 300 nm is negligible and c-Si has no absorption at wavelengths longer than 1200 nm. The photocurrent density corresponding to absorption (either photocurrent gain or loss) in a specific layer ( $J_a$ ) can be estimated from the equation:

$$J_a (\text{mA/cm}^2) = q \int_{1200}^{300} A(\lambda) \phi(\lambda) d\lambda = \bar{A} \times 46.46 \text{ mA/cm}^2. \quad (2)$$

Note that  $46.46 \text{ mA/cm}^2$  is the ideal maximum  $J$  in case that all the photons at wavelengths ranging from 300 nm to 1200 nm of the AM1.5 solar spectrum are absorbed to generate electron and hole pairs, which are then collected without any losses. The weighted fractional reflectance ( $\bar{R}$ ) and the corresponding photocurrent density loss  $J_R$  can be calculated similarly by using the specific reflectance  $R(\lambda)$ . To evaluate the current output of solar modules, we assume that the  $J_a$  of the active layer (the intrinsic a-SiO:H layer for a-SiO:H cells, the CuGaSe<sub>2</sub> layer for CuGaSe<sub>2</sub> cells, the CH<sub>3</sub>NH<sub>3</sub>PbI<sub>3</sub> layer for perovskite cells and the c-Si “layer” for c-Si cells) is equal to the short-circuit current ( $J_{sc}$ ) of the solar cell. Since reflection losses of the module and parasitic absorption losses from layers other than the active layer are taken into account, this assumption is acceptable for estimating  $J_{sc}$  if the thickness of the active layer is smaller than the diffusion length of minority carriers [5, 6] in c-Si and the collection length in the thin film cells (determined by combined drift and diffusion mechanisms). The optical performance of a hybrid tandem module can be evaluated by the sum ( $J_{sc\_sum}$ ) of the  $J_{sc}$  from the top cell ( $J_{sc\_t}$ ) and the  $J_{sc}$  from the bottom cell ( $J_{sc\_b}$ ).

### 3. Results and discussion

#### 3.1 Optical design of hybrid tandem modules

Initial calculation shows that, compared to the IBC module structure in Fig. 1(a), implementation of thin-film solar cells onto the inner side of flat module glass (Fig. 1(b)) drastically increases reflection and parasitic absorption losses of modules, making this hybrid tandem concept difficult to result in a gain in efficiency. The reasons for the increase of reflection losses are that a thin-film solar cell introduces multiple interfaces with contrasting refractive indices of its layers. The thin layers at a scale of  $\sim 100$  nanometers cause strong light interference effects. For example, as shown in Fig. 2(a), the reflection of a hybrid tandem module with a-SiO:H top cells leads to a reflection loss of about  $9 \text{ mA/cm}^2$ , which accounts for 19% of the photons at wavelengths ranging from 300 nm to 1200 nm in the AM1.5 solar spectrum. The intrinsic a-SiO:H layer thickness influences the  $J$  by interference effects. To reduce the reflection loss, a random pyramid-like micrometer-scale texture, replicated from an etched c-Si wafer, can be introduced onto the module glass. In practice it can be realized by imprint lithography [7]. The pyramid-like texture on the module glass can effectively decrease the reflection loss from  $9 \text{ mA/cm}^2$  to  $4 \text{ mA/cm}^2$ , and further down to  $2.5 \text{ mA/cm}^2$  with double-sided texture as shown in Fig. 2(a). Furthermore, the influence of light interference caused by the thin layer is almost eliminated. The schematic layer stack of the hybrid tandem module with the textured module glass is illustrated in Fig. 2(b) and also used in the latter simulation. The major parasitic absorption in the hybrid tandem module originates from the Transparent Conductive Oxide (TCO) layers since in 4-terminal tandem concepts, TCO has to be used as both the front and rear electrodes of the top cell. The free carrier absorption in the near-infrared severely reduces the number of photons that are left for absorption by the c-Si bottom cell. In order to reduce this parasitic absorption of TCO, the hydrogen doped indium oxide (IO:H) material with low free-carrier density and very high mobility, which was published recently [8], is a very promising candidate as a TCO for semitransparent thin film cells and has therefore been used as the TCO of the hybrid tandem module in the modelling for this paper. Layer stacks of different solar cells and layer thicknesses used as input of the simulation are listed in Table 1.

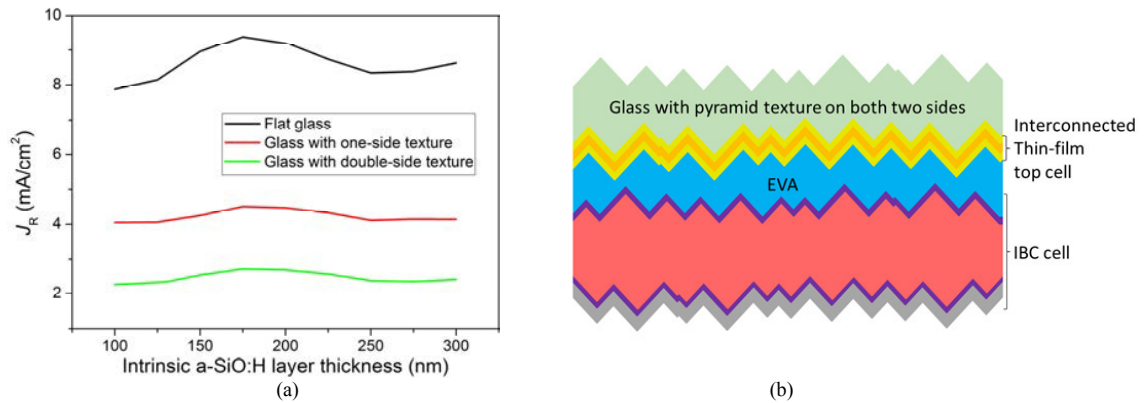


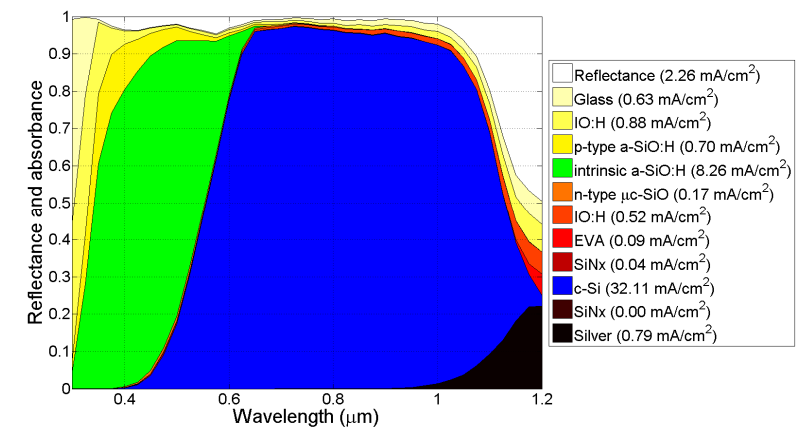
Fig. 2. (a) Reflection losses in terms of the current density for hybrid tandem modules with different glass morphology and different intrinsic a-SiO:H layer thickness and (b) schematic layer stacks of hybrid tandem modules with textured module glass.

Table 1. Layer stack and thickness of different thin-film top cells and c-Si bottom cells used as input of the simulation. Note that there is also 100- $\mu$ m thick EVA between the top and bottom cells.

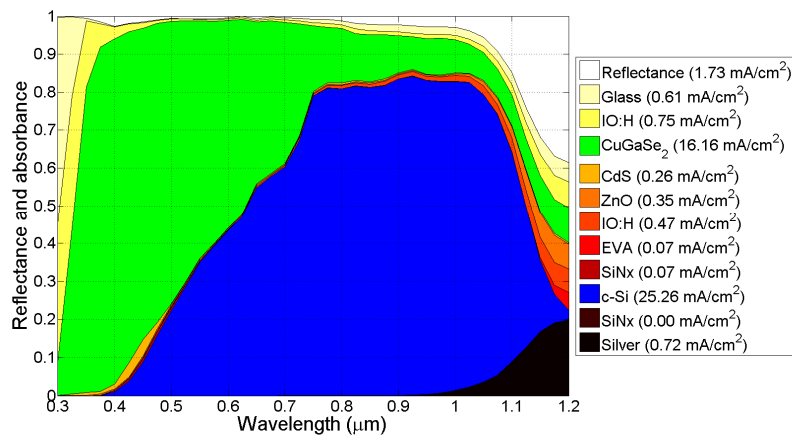
a-SiO:H top cell		CuGaSe <sub>2</sub> top cell		Perovskite top cell		c-Si bottom cell	
Layer	Thickness ( $\mu$ m)	Layer	Thickness ( $\mu$ m)	Layer	Thickness ( $\mu$ m)	Layer	Thickness ( $\mu$ m)
Glass	2000	Glass	2000	Glass	2000	SiN <sub>x</sub>	0.08
IO:H	0.1	IO:H	0.1	IO:H	0.1	c-Si	160
p-type a-SiO:H	0.01	CGS	0.1	Compact TiO <sub>2</sub>	0.1	SiN <sub>x</sub>	0.08
Intrinsic a-SiO:H	0.1	CdS	0.055	CH <sub>3</sub> NH <sub>3</sub> PbI <sub>3</sub>	0.1	Silver	20
n-type $\mu$ c-SiO:H	0.02	ZnO	0.09	Spiro-OMeTAD	0.3		
IO:H	0.1	IO:H	0.1	IO:H	0.1		

The module reflectance and the absorbance of each layer are simulated for three kind of top cells as shown in Fig. 3. The optical simulation in Fig. 3(a) shows that the  $J_{sc\_sum}$  of the hybrid tandem module with an a-SiO:H top cell can reach 40.37 mA/cm<sup>2</sup>. Although the IO:H and doped layers lead to parasitic absorption losses of 1.4 mA/cm<sup>2</sup> and 0.87 mA/cm<sup>2</sup> respectively, the losses from the encapsulating layer of EVA and the passivating layer of SiN<sub>x</sub> become negligible in the presence of the top cell. For the hybrid tandem module with a CuGaSe<sub>2</sub> top cell as shown in Fig. 3(b), the  $J_{sc\_sum}$  is 41.42 mA/cm<sup>2</sup>. The IO:H leads to a parasitic absorption loss of 1.22 mA/cm<sup>2</sup>. Since the light comes from the glass side of the CuGaSe<sub>2</sub> solar cell, CdS and ZnO are located at the rear, leading to a small parasitic loss of 0.82 mA/cm<sup>2</sup>. Note that there is significant absorption at wavelengths longer than 730 nm, although the optical bandgap of CuGaSe<sub>2</sub> is about 1.7 eV. If this is parasitic sub-gap absorption not leading to free carriers, the  $J_{sc\_sum}$  of the hybrid tandem cell with a CuGaSe<sub>2</sub> top cell will be 3.92 mA/cm<sup>2</sup> lower. Further clarity on this sub-gap absorption is needed. Optical simulation of the hybrid tandem module with a perovskite top cell (Fig. 3(c)) shows a high  $J_{sc\_sum}$  of 41.41 mA/cm<sup>2</sup>. The reason for the high  $J_{sc\_sum}$  is that refractive indices of the layers in the perovskite cell do not diverge much, leading to a smaller reflection loss. Furthermore, the compact TiO<sub>2</sub> and Spiro-OMeTAD only cause a small parasitic absorption loss of 0.33 mA/cm<sup>2</sup>.

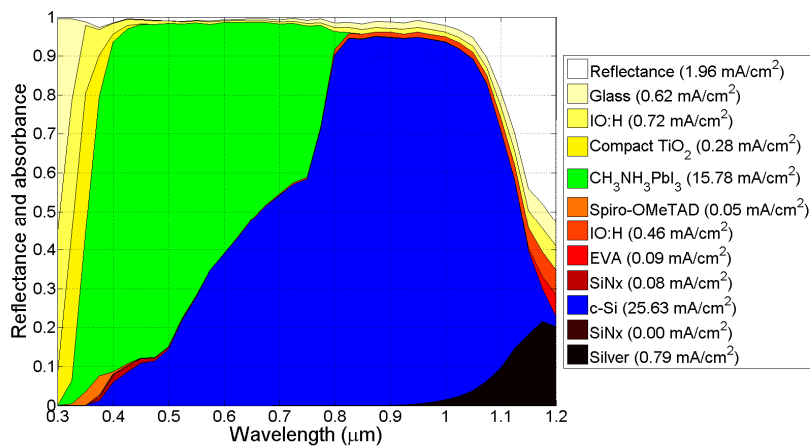
To summarize this section, the hybrid tandem module with the designed texture and high-quality TCO is capable of generating a  $J_{sc\_sum}$  of over 40 mA/cm<sup>2</sup>, which is similar to the  $J_{sc}$  of a high-performance IBC module [1]. This means that no significant optical losses are caused by adding the thin-film cells onto the inner side of the IBC module glass. It should be noted that although the  $J_{sc\_sum}$  is not considerably higher than the  $J_{sc}$  of an IBC cell, this tandem structure represents a large efficiency gain because the charge carriers due to the high energy photons are extracted at higher operating voltage.



(a)



(b)



(c)

Fig. 3. Simulated reflectance and absorbance spectra of 4-terminal hybrid tandem modules with (a) a-SiO:H top cells ( $J_{sc,t}=8.26 \text{ mA/cm}^2$  and  $J_{sc,b}=32.11 \text{ mA/cm}^2$ ), (b) CuGaSe<sub>2</sub> top cells ( $J_{sc,t}=16.16 \text{ mA/cm}^2$  and  $J_{sc,b}=25.26 \text{ mA/cm}^2$ ) and (c) Perovskite top cells ( $J_{sc,t}=15.78 \text{ mA/cm}^2$  and  $J_{sc,b}=25.63 \text{ mA/cm}^2$ ). The  $J$  calculated from the reflectance and absorbance is listed in the legend.

### 3.2 Efficiency estimation of hybrid tandem modules

To evaluate the efficiency gain of a hybrid tandem module,  $V_{oc}$  and  $FF$  changes of the c-Si bottom cell at lower light intensity or smaller  $J_{sc}$  have to be taken into account. With the two-diode equation and the orthogonal distance regression (ODR) fitting method, the  $J$ - $V$  curve of our IBC cell processed at ECN can be fitted to obtain the device parameters such as saturation current, ideality factors, series and shunt resistance. Therefore, the  $J$ - $V$  curve at other light intensities and concomitant  $J_{sc}$  can be deduced. Fig. 4(a) shows how  $V_{oc}$  and  $FF$  of our IBC cell change with  $J_{sc}$ . The product  $V_{oc} \cdot FF$  of the IBC cell is plotted as a function of the  $J_{sc}$  as shown in Fig. 4(b) and the curve is mathematically fitted with a polynomial function so that the IBC cell efficiency can be expressed by  $J_{sc}$  a single variable. Therefore, the efficiency of a hybrid tandem module ( $\eta$ ) with the given IBC bottom cell can be expressed by the equation:

$$\eta(\%) = \eta_t + \eta_b = V_{oc\_t} \cdot FF_t \cdot J_{sc\_t} + J_{sc\_b} \cdot (0.412 + 0.00362 \cdot J_{sc\_b} - 0.0000429 \cdot J_{sc\_b}^2), \quad (3)$$

where  $\eta_t$  and  $\eta_b$  are respectively the efficiency of the top and bottom cells,  $V_{oc\_t}$  and  $FF_t$  are the open-circuit voltage and the fill factor of the top cell. Eq. 3 leads to Fig. 5, assuming that  $J_{sc\_sum}$  is equal to a constant of 40 mA/cm<sup>2</sup>. The dots in Fig. 5 indicate the possible efficiency of a hybrid tandem module that could be achieved by introducing different thin-film solar cells onto the IBC module cover glass, starting from an IBC module with an efficiency of about 19.5%. The  $J_{sc\_t}$  for different thin-film solar cells are taken from Fig. 3 and the product  $V_{oc} \cdot FF$  of three different top cells is taken from the literature [9, 10, 11]. This offers the possibility to make a hybrid tandem module with an efficiency of over 24%. For a-SiO:H and CuGaSe<sub>2</sub> top cells, the absolute efficiency gain will be about 2.5% and 3% respectively. The use of a perovskite top cell can lead to a significant absolute efficiency gain of over 5%.

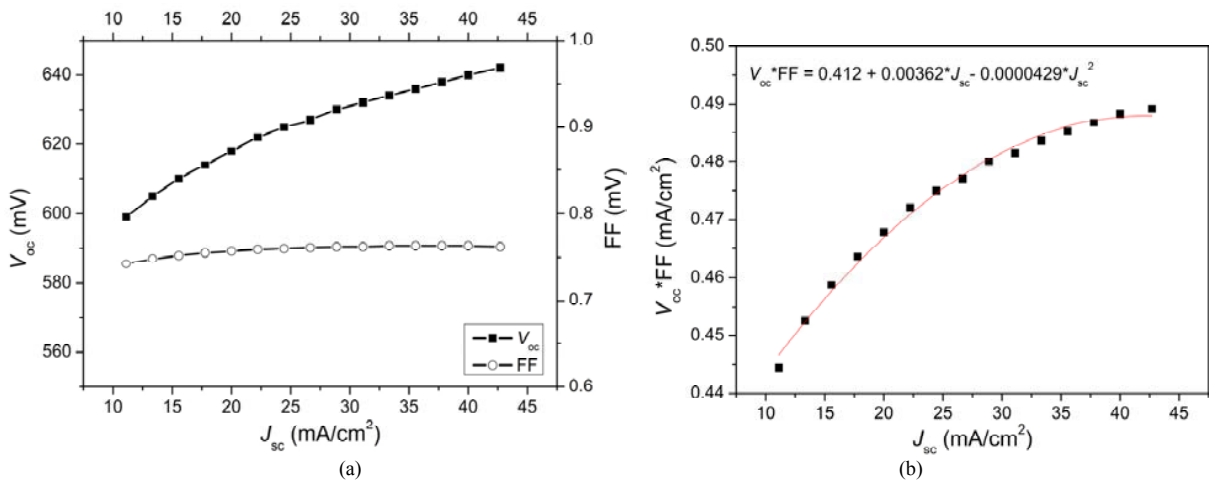


Fig. 4. (a)  $V_{oc}$  and  $FF$  of the IBC cell as a function of  $J_{sc}$  and (b) the product of  $V_{oc} \cdot FF$  as a function of  $J_{sc}$  as well as the fitting equation.

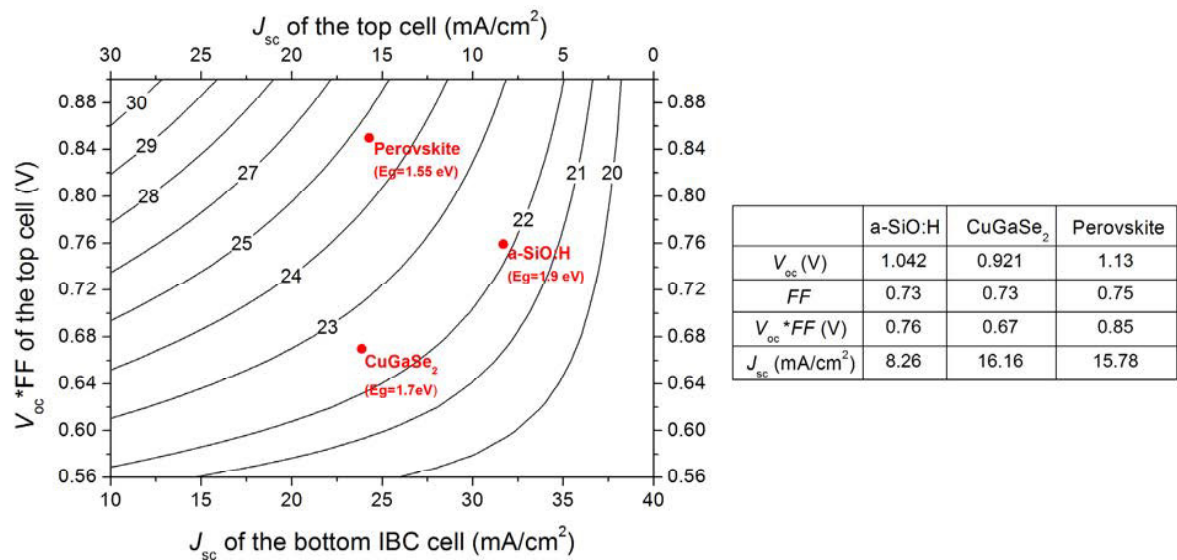


Fig. 5. Possible efficiency (numbers on the curves) of a hybrid tandem module with different thin-film top cells. The  $V_{oc}$ ,  $FF$  and  $J_{sc}$  of the three different top cells are indicated in the table.

#### 4. Conclusion

Our optical simulation and design have shown that it is possible for the hybrid tandem module to generate a  $J_{sc\_sum}$  of over 40 mA/cm<sup>2</sup> by introducing thin-film solar cells onto the module glass of a IBC module. In order to achieve this high current output, the antireflective structure of pyramid-like textures is implemented to the module glass. In addition, IO:H which has good conductivity and very low near-infrared absorption is chosen as the transparent electrode for both front and back of the thin-film top cells. Our methodology to estimate the efficiency of the hybrid tandem module, which is mostly based on practical solar-cell parameters, shows the efficiency increase that three different thin-film technologies can lead to. Starting from a IBC module with an efficiency of 19.5%, the possible efficiency gain is about 2.5% for a-SiO:H top cells and about 3% for CuGaSe<sub>2</sub> top cells. Utilization of a perovskite top cell in a hybrid tandem module can result in an absolute efficiency gain of over 5%. With this structure it is possible to achieve a module efficiency of over 24% with this 4-terminal hybrid tandem module concept using state-of-the-art materials.

#### Acknowledgements

Authors would like to thank Maarten Dörenkämper, Klaas Bakker, Karine van der Werf, and Teun Burgers at ECN for the technical discussions and Rudi Santbergen at Delft University of Technology for the discussion about optical simulation.

#### References

- [1] Green MA, Emery K, Hishikawa Y, Warta W, Dunlop ED. Solar cell efficiency tables (version 43). Prog Photovoltaics 2014; 22: 1–9.
- [2] Masuko K, Shigematsu M, Hashiguchi T, Fujishima D, Kai M, Yoshimura N, Yamaguchi T, Ichihashi Y, Mishima T, Matsubara N, Yamanishi T, Takahama T, Taguchi M, Maruyama E, Okamoto S. Achievement of more than 25 % conversion efficiency with crystalline silicon heterojunction solar cell. IEEE J Photovolt 2014;4:1433–5.
- [3] White T, Lal N, Catchpole K. Tandem solar cells based on high-efficiency c-Si bottom cells: Top cell requirements for >30% efficiency. IEEE J Photovolt 2014;4: 208–14.
- [4] Zeman M, Krc J. Optical and electrical modeling of thin-film silicon solar cells. J Mater Res 2008; 23:889–98.

- [5] Zhang D, Digdaya I, Santbergen R, van Swaaij RACMM, Bronsveld P, Zeman M, van Roosmalen J, Weeber A. Design and fabrication of a SiO<sub>x</sub>/ITO double-layer anti-reflective coating for heterojunction silicon solar cells. *Sol Energy Mater Sol Cells* 2013;117:132–8.
- [6] Si FT, Kim DY, Santbergen R, Tan H, van Swaaij RACMM, Smets AHM, Isabella O, Zeman M. Quadruple-junction thin-film silicon-based solar cells with high open-circuit voltage. *Appl Phys Lett* 2014;105:063902.
- [7] Battaglia C, Escarré J, Söderström K, Erni L, Ding L, Bugnon G, Billet A, Boccard M, Barraud L, De Wolf S, Haug FJ, Despeisse M, Ballif C. Nanoimprint lithography for high-efficiency thin-film silicon solar cells. *Nano Lett* 2011;11: 661–5.
- [8] Macco B, Wu Y, Vanhemel D, Kessels WMM. High mobility In<sub>2</sub>O<sub>3</sub>:H transparent conductive oxides prepared by atomic layer deposition and solid phase crystallization. *Phys Status Solidi- R* 2014;8:987–90.
- [9] Ishizuka S, Yamada A, Fons PJ, Shibata H, Niki S. Structural tuning of wide-gap chalcopyrite CuGaSe<sub>2</sub> thin films and highly efficient solar cells: differences from narrow-gap Cu(In,Ga)Se<sub>2</sub>. *Prog Photovoltaics* 2014; 22: 821–9.
- [10] Zhou H, Chen Q, Li G, Luo S, Song T, Duan H, Hong Z, You J, Liu Y, Yang Y. Interface engineering of highly efficient perovskite solar cells. *Science* 2014; 345: 542–6.
- [11] Kim DY, Guijt E, van Swaaij RACMM, Zeman M. Development of a-SiO<sub>x</sub>:H solar cells with very high V<sub>oc</sub> × FF product. *Prog Photovoltaics* 2015; 23: 671-84.